2006

Determining the Effect of Substitutions at Alanine 47 in Synechococcus Pcc6301 Ribulose-1,5-Bisphosphate Carboxylase/Oxygenase (RUBISCO)

Christopher R. Salyer
Wright State University

DETERMINING THE EFFECT OF SUBSTITUTIONS AT ALANINE 47 IN SYNECHOCOCCUS PCC6301 RIBULOSE-1,5-BISPHOSPHATE CARBOXYLASE/OXYGENASE (RUBISCO)

A thesis submitted in partial fulfillment
of the requirements for the degree of
Master of Science

By

CHRISTOPHER RYAN SALYER
B.S., Wright State University, 2004

2006
Wright State University

WRIGHT STATE UNIVERSITY

SCHOOL OF GRADUATE STUDIES

December 1, 2006

I HEREBY RECOMMEND THAT THE THESIS PREPARED UNDER MY SUPERVISION BY Christopher Ryan Salyer ENTITLED Determining the Effect of Substitutions at Alanine 47 in Synechococcus PCC6301 Ribulose-1,5-bisphosphate Carboxylase/Oxygenase (RubisCO)BE ACCEPTED IN PARTIAL FULFILLMENT OF THE REQUIREMENTS FOR THE DEGREE OF Master of Science.

_____
Stephanie Smith, Ph.D.
Thesis Director

_____
David Goldstein, Ph.D.
Department Chair

Committee on
Final Examination

_____
Mill Miller, Ph.D.

_____
Jim Amon, Ph.D.

_____
Gerald Alter, Ph.D.

_____
Joseph F. Thomas, Jr., Ph.D.
Dean, School of Graduate Studies

ABSTRACT

Salyer, Christopher Ryan. M.S., Department of Biological Sciences, Wright State University, 2006. Determining the Effect of Substitutions at Alanine 47 in Synechococcus PCC6301 Ribulose-1,5-bisphosphate Carboxylase/Oxygenase (RubisCO).

Mutant screening and genetic selection in various organisms have shown that residues far from the active site of ribulose-1,5-bisphosphate carboxylase/oxygenase (RubisCO) can influence catalytic efficiency and CO_2/O_2 specificity. Because RubisCO catalyzes the rate-limiting step of photosynthesis, further study of these sites distant from the primary reaction center may provide the necessary information for engineering an increase in primary productivity of crop plants. In a previously described system of random mutagenesis and bioselection (Smith, 2002), the RubisCO genes from the cyanobacterium *Synechococcus* PCC6301, were randomly mutated and introduced into the photosynthetic bacterium *Rhodobacter capsulatus*. An A47T substitution resulted in a very modest loss of specific activity. However, this mutant was not functional relative to the wild-type when complementation was performed. Since mutants with even lower catalytic activity were able to complement a RubisCO deletion strain

to photoautotrophic growth, it was hypothesized that the A47T mutation affected important kinetic properties of RubisCO. To further explore the role of this residue, A47 in the cyanobacterial enzyme was changed to Glycine and Proline by site-directed mutagenesis. Analysis of the recombinant proteins demonstrated that both mutant enzymes exhibited lower specific activity than the wild-type enzyme when expressed in *E. coli*. To examine the possibility that the decrease in specific activity was due to decreased expression of the mutant enzymes, SDS-PAGE and Western Blots were performed. SDS-PAGE and Western blotting indicated that there was slightly less of the enzyme present for the mutants. This could be the result of decreased synthesis or increased degradation. Native PAGE demonstrated that the G mutant might be a folding-mutant, since it does not have any detectable holoenzyme on non-denaturing PAGE. To further support this hypothesis, there was also a doublet band present in the mutants on non-denaturing PAGE that was not present in the wild-type. Perhaps this additional band is also an indicator of a misfolded large subunit or an indicator that the polypeptides are closely related in structure. However, the proline mutant was able to form a holoenzyme on non-

denaturing PAGE. The results confirm that A47 plays a critical role in the function of RubisCO.

TABLE OF CONTENTS

LIST OF FIGURES

LIST OF TABLES

ACKNOWLEDGMENTS

I am indebted to Stephanie Smith on innumerable levels. Without Stephanie's intelligence, suggestions, and guidance, most of the results reported here would have never existed. She has been a generous mentor and a joy to work for. She has been patient with me as I have slowly learned to become a scientist. I have tried to rise to the standard she sets, and imagine that I will keep trying for the rest of my scientific career.

The distinguished members of my thesis committee (Mill Miller, Jim Amon and Gerald Alter) provided just the right amount of guidance and were always available when I had questions. Discussions with Mike Goodson have been invaluable. Mike assured me that things do not always go right in the laboratory and has been a wonderful sounding-board for ideas. Many thanks are also extended to Dawn Wooley for her constructive criticism, ideas, and training in her laboratory. I would also like to thank past and present members of the Smith Laboratory. My lab mates supported me through all of this tedious work and motivated me to keep pushing forward.

Most of all, I am grateful to my parents, Stephen and Elaine Salyer, along with my wife, Lauren Salyer, for their unending enthusiasm and support over the past two years. They have never stopped believing in me. This research is dedicated to them.

Introduction

Ribulose-1,5-bisphosphate carboxylase/oxygenase (RubisCO; EC 4.1.1.39) is the most abundant enzyme in the world (Ellis, 1979). Approximately 50% of soluble leaf protein is RubisCO (Roy and Andrews, 2000). However, its abundance may serve to compensate for its intrinsic inefficiency. RubisCO is a very sluggish enzyme with a k_{cat} of 2-5 s^{-1} (Horken and Tabita, 1999). RubisCO is a bifunctional enzyme involved in two conflicting pathways (Figure 1). RubisCO can fix carbon dioxide or molecular oxygen, which leads to carbon fixation or the initiation of photorespiration respectively. Together, these properties make RubisCO the rate-limiting step in photosynthetic CO_2 fixation. During carboxylation, RubisCO covalently attaches CO_2 to RuBP to form a 6-carbon intermediate. This beta-keto intermediate is hydrolyzed and RubisCO cleaves the lengthened chain into two identical molecules of 3-phosphoglycerate (PGA). The majority of the PGA produced (5 out of 6) is recycled to build more RuBP and refuel the Calvin Cycle (Farquhar et al., 1980). The remaining PGA molecule is removed from the cycle to produce glucose.

Oxygenation initiates the phoorespiratory pathway that ultimately results in the loss of CO_2 and completely inhibits carboxylation (reviewed by Spreitzer and Salvucci, 2002). The reaction with oxygen results in an intermediate that is hydrolyzed to 1 molecule of phosphoglycerate and one molecule of p-glycolate (Andrews et al., 1971; Bowes and Ogren, 1970). Photorespiration is a wasteful process because PGA is created at a reduced rate and a higher metabolic cost. The catalytically active form of RubisCO is made when activator CO_2 reacts with the ε-amino group of lysine 201 within the active site of the enzyme (Lorimer and Miziorko, 1980). The CO_2 added to the lysine for carbamylation is not the same CO_2 that is used as a substrate (Lorimer et al., 1976). The resulting carbamate participates in coordination of Mg^{2+} cofactor to form the activated complex (Pon et al., 1963; Lorimer and Miziorko, 1980).

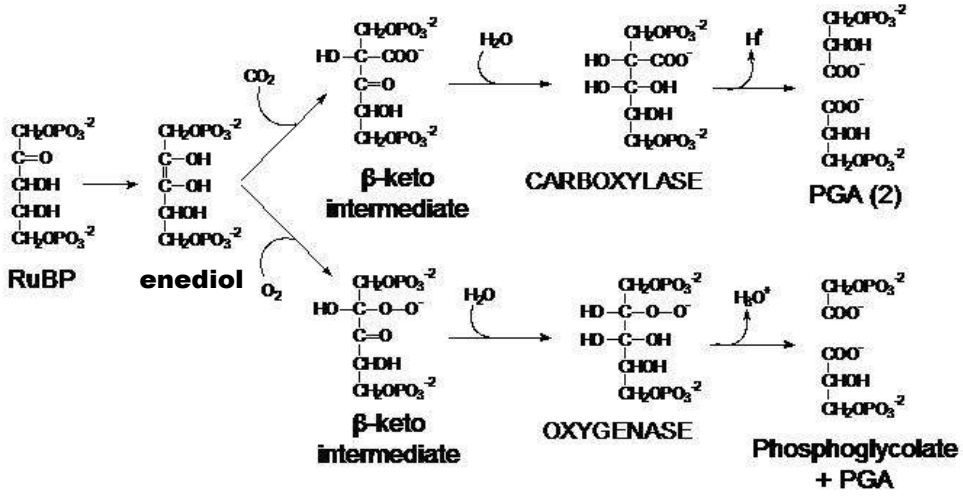

Figure 1. The oxygenation and carboxylation of RuBP catalyzed by RubisCO. The carboxylase activity generates two molecules of 3-phosphoglycerate. The Oxygenation of RuBP leads to the production of one molecule of 3PGA and one molecule of phosphoglycolate, a two-carbon compound which is salvaged in the photorespiratory pathway.

Two predominant RubisCO forms exist in nature—but up to four forms are defined in the literature. Form I RubisCO, which is found in cyanobacteria, phototrophic and chemoautotrophic proteobacteria, and practically all eukaryotic photosynthesizers(reviewed by Andersson and Taylor, 2003), is composed of eight large catalytic subunits (LSU; 55 kDa each) and eight small subunits (SSU; 14 kDa each). The subunits are arranged in a hexadecameric structure (Figure 2 and 3) such that eight large subunits

are arranged in an octameric core surrounded by two layers of small subunits with each layer on opposite sides of the core (Newman and Gutteridge, 1993). The large subunits have a catalytic function whereas the small subunits function is unknown although they are required for full enzyme activity (Andrews and Ballment, 1983). Perhaps the small subunits serve to stabilize the large subunit dimers. The Form I holoenzyme (L8S8) has a total molecular weight of about 550 kDa. Form I RubisCOs can be further subdivided into two major forms: red-like and green-like (Horken and Tabita, 1999). Green-like RubisCOs include those from green plants, green algae, and cyanobacteria, whereas the red-like RubisCOs originate from red algae and purple bacteria (Tabita, 1999).

The more simplistic Form II RubisCOs, which are found only in purple nonsulfur photosynthetic bacteria, lack small subunits and consist exclusively of multiples of large subunit dimers. Form II RubisCOs show only 25 to 30% identities to Form I large subunits (Kellogg and Juliano, 1997). In addition to the Form I and Form II enzymes, two novel types, Form III and Form IV RubisCO also exist (Tabita, 1999). Form III is the "archael" RubisCO and has been previously described (Watson et al., 1999). The Form III RubisCOs are a combination of Form I and Form II

RubisCO and consist of 5 LSU dimers (Maeda et al., 1999). Form IV RubisCOs are the "RubisCO-like proteins" which lack the active site (Hanson and Tabita, 2001).

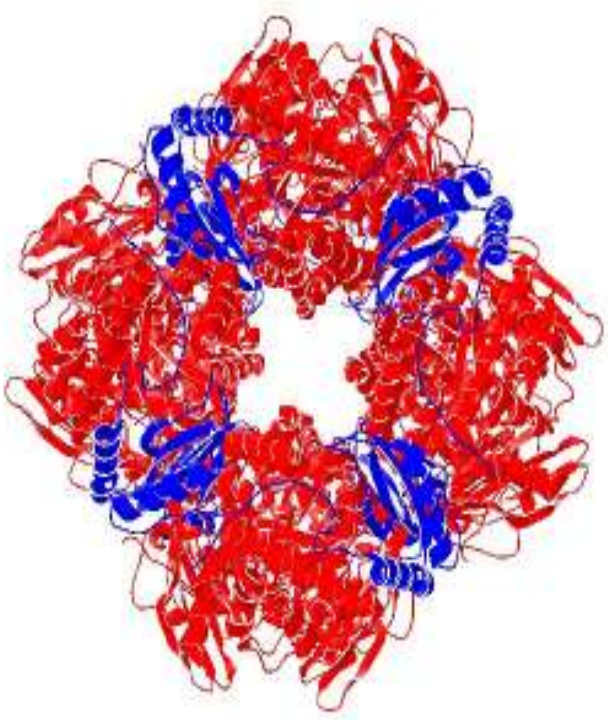

Figure 2. Top-down view of the octameric core of RubisCO from Synechococcus PCC6301. The LSU monomers are each colored red and the SSU monomers are colored blue. In the center of the molecule, there is a solvent channel. This image was created using DeepView in the Swiss Protein Database Viewer, version 3.7b2.

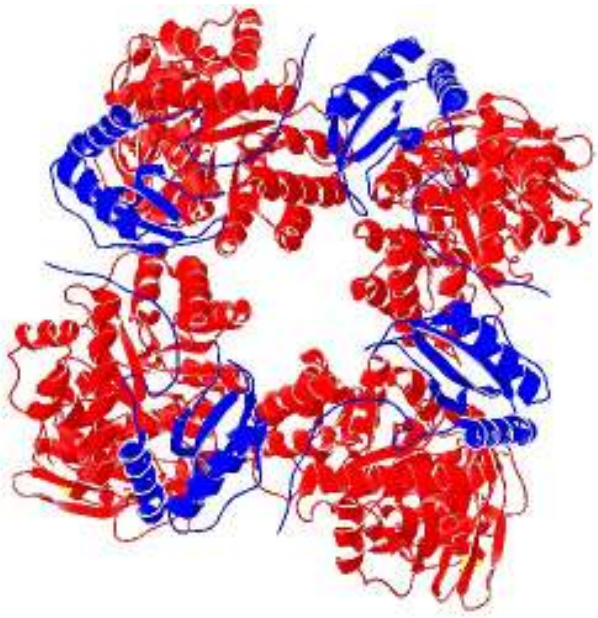

Figure 3. A view-down the 4-fold axis of Synechococcus PCC6301. The trace for only half the molecule (L_4S_4) is shown for clarity. The L-subunit monomers are colored red, and the small subunits are blue. The yellow shows the position of residue 47 (A47). In the center of the molecule, there is a solvent channel. This image was created using DeepView in the Swiss Protein Database Viewer, version 3.7b2.

In hopes of better understanding the structure and function of RubisCO, much attention has been given to X-ray crystallographic structures of the enzyme. More than 20 x-ray crystallographic structures for various RubisCO enzymes now exist within the Protein Data Bank (Berman et al., 2000; Table 1). These structures revealed that the large subunits had two separate domains, an N-terminal domain which included amino acids 1 to 150 and a C-terminal domain which included residues 151 to 475 (Figure 3). Most of the catalytic residues reside within the C-terminal domain.

However, there also exist active-site residues in the N-terminal domain of an adjacent large subunit. The minimal functional unit of RubisCO is a large subunit dimer (L_2) which is in a head-to-tail arrangement (Figure 4), that is, the N-terminus of one subunit interacts with the C-terminal domain of a neighboring large subunit. There are therefore two active sites at the interface of the large subunits in each dimer. The catalytically active form of RubisCO is made when activator CO_2 reacts with the lysine-201 (the numbering is based on the sequence of the spinach enzyme) within the active site of the enzyme.

Figure 4. Position of residue A47 within the large subunit. This image was created using DeepView in the Swiss Protein Database Viewer, version 3.7b2. The red shows the large subunit monomer. The yellow shows the position of A47 in the N-terminal region of the enzyme. The N and C terminal ends of the enzyme are labeled.

Table 1. Examples of Crystal Structures of RubisCO. Most studies on the structural organization of Rubisco have been conducted using X-ray crystallographic analyses.

SOURCE	ORGANISM TYPE OR COMMON NAME	FORM	REFERENCE
Rhodospirillum rubrum	Purple Bacterium	II	Schneider et al., 1986
Chlamydomonas reinhardtii	Green Algae	I	Taylor et al., 2001
Galderia partita	Red Algae	I	Sugawara et al., 1999
Synnechococcus PCC6301	Cyanobacterium	I	Newman and Gutteridge, 1993
Spinacea oleracea	Plant/spinach	I	Andersson et al., 1989; Andersson, 1996
Nicotiana tabacum	Plant/tobacco	I	Chapman et al., 1988
Wautersia eutropha	Soil bacterium	I	Hansen et al., 1999
Chlorobium tepidum	Green Sulfur Bacterium	IV	Li et al., 2005

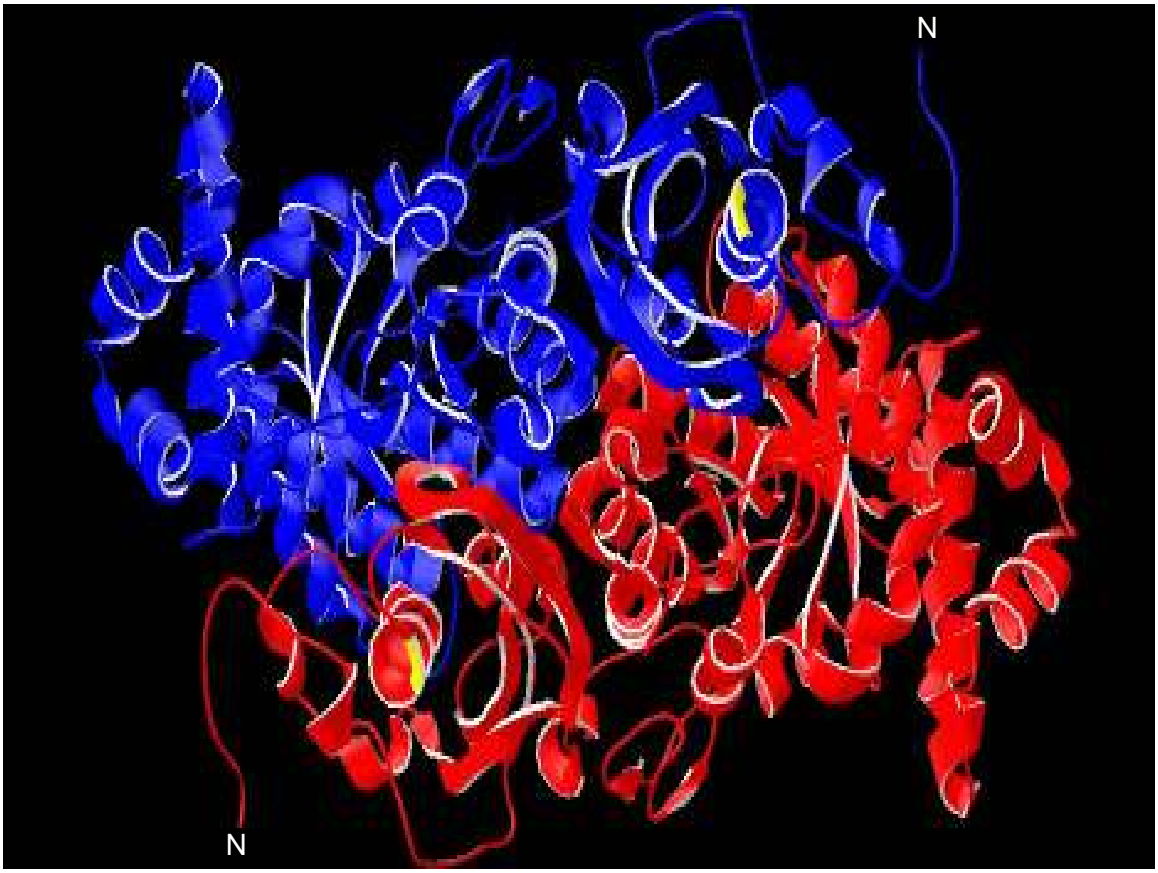

Figure 5. A dimer of large subunits. This image was created using DeepView in the Swiss Protein Database Viewer, version 3.7b2. The large subunit monomers are colored red and blue. The yellow shows the position of A47 in each of the monomers. The N-terminal domain of each LSU is also labeled.

RubisCO shows a considerable lack of CO_2 specificity, defined as the ability of RubisCO to distinguish between CO_2 and oxygen. A high specificity value indicates greater specificity for CO_2. However, a higher specificity value does not necessarily reflect a better carboxylase *in situ*. The ratio of carboxylation to oxygenation at any specified concentrations of CO_2 and O_2 is referred to as the

specificity factor, $\Omega = V_cK_o/K_cV_o$ where V_c and V_o are the maximal velocities for carboxylation and oxygenation respectively, and K_c and K_o are the Michaelis-Menten constants for CO_2 and O_2. In this equation, the substrate specificity determines the relative rate of carboxylation to oxygenation at any CO_2 and O_2 concentrations (Jordan and Ogren, 1981). Cyanobacteria and green algae have a carbon concentrating mechanism (CCM) that reduces the importance of the specificity factor *in vivo* and allows them to fix carbon quite well (Kaplan and Reinhold, 1999). The primary function of the CCM is to transport high levels of CO_2 to the active site.

The major objective of many RubisCO researchers is to alter the specificity factor in favor of carboxylation, in hopes of increasing primary productivity in crop plants. Altering the specificity factor is rather complicated since neither CO_2 nor O_2 binds directly to the active site. The specificity factor has increased during evolution to compensate for the gradual atmospheric shift from high CO_2 and low O_2 to low CO_2 and high O_2 (Jordan and Ogren 1981). The present CO_2/O_2 ratio is believed to have existed for the past 60 million years (Ehleringer et al., 1991). What then has stalled RubisCO's adaptation to the current environment? Perhaps RubisCO was best able to adapt to low

atmospheric CO_2 by increasing the specificity for CO_2. The high oxygen concentrations probably prohibited speedy adaptation of the catalytic center to reduce or eliminate oxygenase activity. The comparison of specificity values, which vary over a 20-fold range from divergent photosynthetic organisms (Table 2), supports this hypothesis. The specificity has overall increased during evolution from around 40 for cyanobacteria to around 80-250 for higher plants and red algae. In general, Form I enzymes have higher specificities than Form II enzymes (reviewed in Tabita, 1999). Such variations suggest that it is possible to alter the enzyme to favor the specificity for CO_2 and enhance the specific activity. Thus, scientists present a credible case in potentially accelerating the evolution of RubisCO in the laboratory.

Table 2. Comparison of specificity values from divergent photosynthetic organisms.

SOURCE	FORM	Ω	Reference
Nicotiana tabacum	I (green)	77+/-1	Jordan and Ogren (1981)
Nicotiana tabacum	I (green)	82	Whitney et al. (2001)
Spinacea oleracea	I (green)	80+/-1	Jordan and Ogren (1981)
Spinacea oleracea	I (green)	82	Kane et al. (1994)
Chlamydomonas reinhardtii	I (green)	61+/-5	Jordan and Ogren (1981)
Chlamydomonas reinhardtii	I (green)	60+/-1	Du et al. (2003)
Synechococcus PCC6301	I (green)	43	Kane et al. (1994)
Rhodobacter capsulatus	I (green)	25.9+/-0.96	Horken and Tabita (1999)
Hydrogenovibrio marinus	I (green)	25	Igarashi and Kodama (1996)
Anaebaena 7120	I (green)	35	Larimer and Soper (1993)
Galdieria partita	I (red)	238+/-9	Uemura et al. (1997)
Alcaligenes eutrophus	I (red)	75	Lee (1991)
Rhodobacter sphaeroides	I (red)	62	Jordan and Ogren (1981)
Bradyrhizobium japonicum	I (red)	75	Horken and Tabita (1999)
Cyanidium caldarium	I (red)	225	Uemura et al. (1997)
Rhodospirillum rubrum	II	15+/-1	Jordan and Ogren (1981)
Rhodospirillum rubrum	II	12.3	Kane et al. (1994)
Thiobacilus denitrificans	II	14+/-0.8	Hernandez et al. (1996)

Many researches have taken a mutagenic approach to improve RubisCO by investigating the regions and amino acid residues that influence the catalytic properties of the enzyme. Perhaps it is tempting to consider the active site residues the most obvious targets for improvement of RubisCO. Because these active-site residues are nearly 100% conserved (Read and Tabita, 1994), they simply do not explain the discrepancy in kinetic parameters observed between RubisCO enzymes from different species. Furthermore, mutagenesis of these residues so far has not led to an improvement in specificity.

Perhaps the most studied region of the enzyme is the highly conserved loop 6 region of the large subunit. The loop 6 region is hypothesized to move and lock substrates in the active site (Andersson, 1996) in a closed conformation. This closed conformation is important and could be the rate-limiting step of catalysis. The first clue that this region was important was when Chen and Spreitzer (1992) mutated Valine 331 in RubisCO from *Chlamydomonas* to an alanine. This mutation decreased the specificity factor by almost 40%.

The N-terminal region of the enzyme does not show the same level of conservation as the loop 6 region and is quite divergent among species. These differences might be of interest in regard to catalysis (reviewed in Schneider et al., 1992). The N-terminal region is of interest because of its requirement for catalytic competence. Removal of the first eight residues of the N-terminal end in spinach (Houtz et al., 1989) RubisCO does not affect catalytic activity, whereas removal of six additional residues drastically reduces catalytic activity. In a similar study, a 90% loss of activity was reported when residues 9-14 of the N-terminal end were removed from the LSU of wheat RubisCO (Gutteridge et al., 1986). Thus, the

N-terminal region may be important in maintaining catalytic activity.

Given the lack of success with directed mutagenesis of residues in and proximal to the active site (Spreitzer et al., 1988; Bainbridge et al., 1998), the more promising approach for improving Rubisco is to investigate residues and regions that are farther from the active site (Spreitzer, 2002; Smith, 2002; Satagopan and Spreitzer, 2004; Smith and Tabita, 2003; Watson and Tabita, 1997; Andrews and Whitney, 2003). Study of these distant interactions may provide the necessary information for engineering an increase in the agricultural production of food and renewable energy. It has also become increasingly important to study even lethal mutations and investigate the structural alteration induced by these mutations to increase our knowledge of structure-function relationships. Many mutants have been selected and biochemically characterized, but the structural role of most of the mutated residues has not been determined.

The aim of this thesis is to better understand the role Alanine 47 in *Synechococcus* PCC6301 (*Anacystis nidulans*) plays in protein structure and function. This enzyme was chosen because of its high sequence and structural identity to plant enzymes (Shinozaki and

Sugiura, 1983), because of its ease of assembly into an L_8S_8 holoenzyme in *E. coli*, because its crystal structure is published (Newman and Gutteridge, 1993), and ease of mutagenesis studies (Tabita, 1999; Tabita and Small, 1985). Collectively, these characteristics make *Synechococcus* PCC6301 a suitable model for the higher plant enzyme.

In a previous study, random mutagenesis resulted in a substitution at residue 47 that was shown to affect the activity of the *Synechococcus* PCC6301 RubisCO. The threonine substitution resulted in 80% activity retained in the mutant, relative to the wild-type (Smith, 2002). However, this mutant form of the enzyme was unable to complement a RubisCO deletion host, *R. capsulatus* SBI-II$^-$, to RubisCO-dependent growth. It is possible that a kinetic property of the enzyme was affected, since the enzyme was shown to properly assemble into a holoenzyme, and there was no apparent decrease in its levels in the cell. Based upon these previous results, it was hypothesized that, since mutants with even lower catalytic activity were able to complement the RubisCO-deletion strain to photoautotrophic growth, perhaps an important kinetic parameter, such as the affinity for CO_2, had been affected in the A47T mutant. The affinity for CO_2 is an important property in that it is very low for this particular RubisCO, probably because it is

normally found in the context of a carbon concentrating mechanism.

Guided by crystallographic structural information (Andersson, 1996) and these previous findings (Lee et al., 1993; Smith and Tabita, 2002), Alanine-47 of the large subunit from *Synechococcus* PCC6301 RubisCO was mutated to either glycine or proline. These mutants were made far from the active site in Alpha-helix 2 of the N-terminal end of the large subunit. Alanine was mutated to a glycine in hopes of making a conservative substitution, and because it is common in alpha helices (Javadpour, 1999). Residue 47 was also chosen because it is highly conserved, typically as a proline, in RubisCO across taxa (Fig. 6).

Residue #	42	43	44	45	46	47	48	49		
Wautersia eutropha	Q	D	G	V	D	**P**	V	E	Red-Like	Ω=75
Bradyrhizobium japonicum	Q	E	G	V	D	**P**	I	E	Red-Like	Ω=75
Xanthobacter flavus	H	D	G	G	P	**P**	V	C	Red-Like	Ω=44
Synechococcus PCC6301	Q	P	G	V	P	A	D	E	Green-Like	Ω=43
Spinacea oleracea	Q	P	G	V	P	**P**	E	E	Green-Like	Ω=80

Figure 6. Protein multiple sequence alignment. Protein multiple sequence alignment using CLUSTALW, followed by Expasy translate tool to convert amino acid sequences to Protein sequences. Only residues 42-49 are shown with the proposed residue of interest, Alanine 47, listed in bold along with its conserved sequences. Accession numbers used are as follows: *Wautersia eutropha* (U20584), *Bradyrhizobium japonicum* (AF041820), *Xanthobacter flavus* (Z22705), *Synechococcus* PCC6301 (X03220), and *Spinacea oleracea* (PF00016).

This thesis will examine the importance of residue A47 in *Synechococcus* PCC6301 RubisCO. Mutations A47P and A47G were hypothesized to severely impair the enzyme's function, either through an effect on holoenzyme assembly or an effect on kinetic properties. The first part of the experiments presented herein was to determine the specific activities (nmol CO_2 fixed/minute/mg protein) of the wild-type and mutant enzymes in crude extracts of *E. coli*. Secondly, the expression of the wild-type and mutants was examined and conclusions can be drawn as to whether the specific activity correlates with the expression of the enzyme. Next, the ability of the mutants and wild-type to properly fold and form a functional holoenzyme (L_8S_8) will be examined by nondenaturing gels and molecular modeling. Lastly, Western Blots of denaturing gels were performed to confirm that the bands we called LSU in the above gels were actually the RubisCO large subunit and to quantitatively assess the expression levels of that protein.

Materials and Methods

Bacterial Strains and Plasmids

Plasmid pBGL710 (Lee and Tabita, 1991) is a medium-copy (30) number plasmid containing the RubisCO genes (*rbcL* and *rbcS*) from *Synechococcus* strain PCC6301. *E. coli* containing this plasmid is referred to as the wild-type in these studies. Plasmid pBGL710 was transformed into *E. coli* JM109, which was grown in Luria-Bertani (LB) medium. LB media was made with 10 g of Bacto-Tryptone, 5 g of Bacto-yeast extract, 10 g of NaCl and distilled water to 1 L (pH 7.5). To maintain selective conditions for pBGL710, the agar and liquid media contained 50 µg/ml of ampicillin.

Site-directed Mutagenesis

Complementary primers (Table 3) were used to construct the site-directed mutants with the Quik-Change kit from Stratagene (Stratagene, La Jolla, CA) using pBGL710 as the template. This and all subsequent PCR reactions were carried out in a BioRad I-cycler (BioRad, Hercules, CA). Control and sample PCR reactions were prepared according to the manufacturer's instructions. Mutagenesis reactions were

performed under the following cycle conditions: 95°C denaturation and enzyme activation for 1 min followed by 12 cycles of 95°C denaturation for 30 s, 55°C annealing for 1 m and 68°C extension for 5 m. The PCR reactions were then allowed to cool to 4°C before *DpnI* was used to digest the methylated, nonmutaed parental DNA template. The PCR DNA (4 µl) was then added to 50µL thawed XL1-Blue cells and incubated on ice for 30 minutes, after which they were heat pulsed at 42°C for 45 seconds and placed back on ice for 2 minutes. SOC broth (20 g/l Tryptone, 5 g/Yeast Extract, 0.5 g/l NaCl) was preheated to 42°C, and 0.5 mL was added to each tube. After one-hour incubation at 37°C with shaking, the cells were plated onto LB-AXI plates and incubated at 37°C overnight. IPTG and X-gal were added for blue-white screening.

Table 3. Mutagenesis Primers. The bases that introduce the mutations are underlined.

Primer	**Strand**	**Orientation**
A47G	reverse	5′ CCAGCTTCGTCACCAGGGACACCCG-3′
A47G	forward	5′-CGGGTGTCCCTGGTGACGAAGCTGG-3′
A47P	reverse	5′-CCAGCTTCGTCAGGAGGGACACCCG-3′
A47P	forward	5′-CGGGTGTCCCTCCTGACGAAGCTGG-3′

Plasmid purification by QiaPrep Mini-Prep Kit.

For each mutant constructed, a single colony was selected from the Quik-change plates and transferred, with

a sterile toothpick, into 2 mL LB-Amp media for overnight growth in a 37°C shaker. The next day, cells were harvested by centrifugation. Excess medium was removed, and putatively mutated pBGL710 plasmids were isolated with the Qiaprep Miniprep kit (Qiagen, Valencia, CA), and stored at -20°C. Restriction digests with *Eco*R1 (Promega, Madison, WI) were run on 0.8% agarose gels to identify a linearized plasmid of appropriate size.

DNA Quantitation and Sequencing

The plasmids preps were examined for DNA concentration using a Nanodrop ND-1000 Spectrophotometer (Nanodrop Technologies, Wilmington, DE). The mutations and wild-type were verified by sequencing with a CEQ 8000 Genetic Analysis System (Beckman Coulter, Fullerton, CA). The wild-type was sequenced prior to construction of the mutants to verify that our template had the correct amino acid sequence. The sequencing reactions were performed using the GenomeLab Methods Development Kit (Beckman Coulter, Fullerton, CA). In order to completely sequence both strands of the DNA for the entire region, seven primers (Table 4) were routinely used in addition to the M13 Universal forward and reverse primers.

Table 4. Sequencing Primers. Primers were used to verify that the mutations made with the Quik-Change kit were made correct. In addition, primers were used to verify that no other mutations or alterations were present in the rest of the enzyme. All of the sequencing primers were supplied by (Fisher Scientific, Pittsburgh, PA).

Primer	Orientation
PCC6301A	5′-TCTCCCCCAGCCTTTCGACTT-3′
PCC6301B	5′-CCCCCAGCGATAGTCAGAGGCTCC-3′
PCC6301C	5′-GGGGTGACCCAAGGTGCCGCCACC-3′
PCC6301D	5′-GGTCGGCGCGGTCACGTTCAGGTAGTGACC-3′
PCC6301E	5′-GGTCGAGCGGGTAAGCGATGAACG-3′
PCC6301F	5′-CCGCTTCCCCGTCGCCTTGGTCAAAACCTTCC-3′
PCC6301G	5′-GGTGCCGCGACAACGGCGTCCTGC-3′

Cell culture and Preparation of cell extracts

E. coli strains harboring pBGL710 were grown at 37°C overnight in 2 ml of Luria-Bertani (LB) medium containing 100 µg/ml ampicillin; 250 µl of this culture was used to inoculate each of four flasks containing 25 ml of LB containing 100 µg/ml ampicillin. For expression of RubisCO genes, 100 mM isopropyl B-D-thiogalactopyranoside was added to a final concentration of 0.5 mM IPTG after 3 hours of growth. The OD at the time of induction was measured at 595 nm using a Milton Roy Spectronic 401 (Milton Roy, Ivyland, PA). After induction, cultures were incubated at 37°C with shaking for 8 hours prior to harvesting.

Cultures were placed in sterile 50 ml Oakridge tubes and centrifuged 5 minutes at 10,000 x *g* at 4°C in an Avanti J-26 XPI centrifuge (Beckman Coulter, Fullerton, CA) to

collect cells. Harvested cells were resuspended in 10 ml of 100 mM Tris-HCl, 1 mM EDTA, pH 8.0 (TE) and centrifuged again for 5 minutes at 10,000 x g at 4°C. Supernatant was removed and samples were resuspended in 2 ml of TE and then aliquoted into 1 ml cultures in 1.5 ml Eppendorf tubes. Resuspended samples were centrifuged again for 5 minutes at 10,000 x g. The supernatant was removed and the remaining cell pellets were stored at -20°C until they were assayed.

Preparation of Cell Extracts and assays

Prior to assays, frozen cells were thawed on ice, and resuspended in TE containing 5 mM β-mercaptoethanol. Cells were either disrupted by sonication or permeabilized by the addition of the permeabilization agent hexadecyltrimethylammonium bromide (CTAB, Sigma, St. Louis, MO) to a final concentration of 0.025% (w/v) for whole-cell assays. Permeabilized cells allow the passage of substrates through the cellular wall and membrane.

Protein Quantification

The protein concentration was determined by either the Lowry Method (Lowry et al., 1951), the Bradford procedure (Bradford, 1976), or using the CB-X Protein Assay Kit (G-Biosciences, St. Louis, MO). All methods lead to a change in absorbance when protein is present. The Lowry Assay was

performed as a modification to the original protocol (Markwell, 1978). The original Lowry method has been modified by the addition of SDS in the alkali reagent and an increase in the amount of copper tartrate reagent. These modifications allow the method to be used with membrane and lipoprotein preparations without prior solubilization or lipid extraction. One hundred parts of reagent A (2.0% Na_2CO_3, 0.4% NaOH, 0.16% sodium tartrate and 1% SDS) were mixed with one part of reagent B (4% $CuSO_4$ * $5H_2O$) to form reagent C, the alkaline copper reagent. A standard curve was prepared with known protein concentrations. Bovine serum albumin (BSA) was dissolved in distilled water to a concentration of 10 mg/ml. A standard calibration curve was prepared in 1 ml of water with final BSA concentrations from 10-8o µg/ml. A blank (a tube without any protein) was also included. Since the final volume of the standard samples and the unknown samples are the same, the final concentration of the unknown samples was calculated from the least squares line of the standard curve. The blank, which does not include the standard protein, was made up of the same buffer as in the samples. The blank was used to set the spectrophotometer to zero absorbance.

To a volume of 1 ml water, 10 µl of sample was added to replicate one and 20 µl of sample was added to replicate two so that each sample was performed in duplicate. To

each sample, 3 ml of reagent C was then added and mixed by inversion. The samples were then incubated at room temperature for 60 minutes prior to the addition of 0.3 ml of Folin-Ciocalteu (Sigma, St. Louis, MO) reagent (on the day of use, Folin-Ciocalteu reagent was diluted 1:1 with distilled water). Samples were mixed immediately by inversion with each addition. Color was allowed to develop for 45 minutes at room temperature and the absorbance measured at 660 nm using a Beckman Coulter DU800 Spectrophotometer (Beckman Coulter, Fullerton, CA).

For the Bradford Assay, five standard dilutions were prepared to build a calibration curve. BSA was dissolved in distilled water to a concentration of 10 mg/ml. A standard calibration curve was prepared in 1 ml of Bradford Reagent with final BSA concentrations from 1-8 µg/ml. A blank with only 1 ml of Bradford Reagent was also included. The standard calibration curve was plotted as the absorption values versus the concentration of the standards. The concentration of protein sample can then be determined by fitting the measured absorbance value to the standard calibration curve. The Bradford Reagent (BioRad, Hercules, CA) was prepared by adding 5 ml of the concentrated Reagent to 20 ml of distilled water. To every sample cuvette, 1 ml Bradford Reagent was added. Samples

were performed in duplicate with 5 µl of sample being added to replicate one and 10 µl of sample added to replicate two. All cuvettes were then mixed by pipetting up and down and incubated at room temperature for 5 minutes. The absorbance was then measured at 595 nm using a Beckman Coulter DU800 Spectrophotometer (Beckman Coulter, Fullerton, CA). Once the sample solutions were measured by UV/VIS, the concentration was converted from µg/ml into mg/ml (1000 µg/ml) to calculate the true concentration of the sample.

The CB-X protein assay (G-Biosciences, St. Louis, MO) was used to estimate protein concentration for Western Blotting exclusively. It was chosen simply to see if it would work since it gives a quick estimate of protein concentration without preparing protein standard calibration plots. The assay was performed as according to the manufacturer's instructions. Briefly, 5-100 µl of protein sample was added into a 1.5 ml centrifuge tube. CB-X, prechilled at -20°C, was added to the tube and mixed by pipetting. The tube was then centrifuged at 16,000 g for 5 minutes. Following centrifugation, all of the CB-X was removed without disturbing the protein pellet. The protein pellet was then dissolved by adding 50 µl of CB-X Solubilization Buffer-I and 50 µl of CB-X Solubilization

Buffer-II to the tube and vortexing. After vortexing thoroughly, 1 ml of CB-X Assay Dye was added to the tube and the sample was vortexed again. The sample was then allowed to incubate for 5 minutes at room temperature. The absorbance was then measured at 595 nm using a Beckman Coulter DU800 Spectrophotometer (Beckman Coulter, Fullerton, CA). The CB-X table for spectrophotometric results was then used to determine the amount of protein in the sample. The protein concentration (µg/µl) was calculated by dividing the amount of protein (µg) by the protein sample volume (µl).

Radiometric RubisCO assay

Carboxylase activity was measured by $^{14}CO_2$ incorporation into acid-stable 3-phosphoglyceric acid (Whitman and Tabita, 1976). Specific activity of the enzyme was defined as nmol CO_2 fixed/min/mg total protein. Specific activity can be measured by incubating Rubisco with CO_2 and Mg^{2+} to fully carbamylate the enzyme. Sodium bicarbonate was used as the source of CO_2 and was ^{14}C-labeled in this assay. The assay buffer contained 80 mM NaOH *N*-(2-hydroxyethyl) piperazine-*N'*-(2-ethanesulfonic acid) (HEPES)-NaOH, pH 8.0, 50 mM $NaHCO_3$, and 25 mM $MgCl_2$. All assays were performed in liquid scintillation vials in a 30°C water bath in a fume hood. A staggered-timing method was used so that each assay incubates for 5 minutes with

each additive. There were two replicates plus a control for each sample. For the controls, RuBP was not added to the reaction. The substrate consisted of 8 mM RuBP pH 6.8 that initiated the reaction. The assays were terminated by the addition of 2 N Hydrochloric acid (HCl). The vials were then left in the fume hood for at least an hour while unincorporated CO_2 escaped. The assays were then dried in a vacuum oven overnight at 60°C. Samples were resuspended in 200 µl of 2.0 N HCl to remove unbound residual bicarbonate and placed into 3 ml of Ecolite (+) scintillation cocktail (MP Biomedicals, Solon, OH). The amount of label in the PGA end-product is a direct measure of the total amount of RubisCO in the extract. Radiolabeled ^{14}C was detected using a Packard 1900TR liquid scintillation counter.

SDS-PAGE

Sodium dodecyl sulfate-polyacrylamide gel electrophoresis (SDS-PAGE) was performed according to a method previously described (Laemmli, 1970). Laemmli discontinuous gels of 10% acrylamide were prepared with tetramethylethylenediamine (TEMED) and ammonium persulfate (APS) added to polymerize the mixtures. The stacking gel of 4% acrylamide was also polymerized chemically. Prior to loading, samples were heated on a hot block at 60°C for 5 minutes to completely denature the protein. Samples were then centrifuged briefly for 1 minute to collect the

condensate. Standards for molecular weight determination were also prepared in the same way. To each lane, 10 µg of protein was added. Electrophoresis was carried out at 175V for two gels (125V for one gel) until the bromophenol blue marker reached the bottom of the gel (about 2 hours). Proteins were detected by staining with Coomassie brilliant blue R-250 for about 1 hour. The gel was then allowed to destain in methanol/glacial acetic acid solution overnight for visualization of the bands. The identity of the large subunit was confirmed by co-electrophoresed precision plus protein standards (BioRad, Hercules, CA).

Native PAGE

Native PAGE was performed to determine proper assembly of the holoenzyme. With native PAGE, there is no pre-treatment of proteins with SDS before electrophoresis. Proteins will retain their normal shape and charge. Samples were not heated to denature the protein as we were looking for assembly. Laemmli discontinuous gels of 6% acrylamide concentration were prepared with tetramethylethylenediamine (TEMED) and ammonium persulfate (APS) added to polymerize the mixtures. The stacking gel of 4% acrylamide was polymerized chemically as in the same way for the stacking gel. To each lane, 10 µg of protein were added. Electrophoresis was carried out at 175V for two gels (125V for one gel) until the bromophenol blue

marker reached the bottom of the gel. The holoenzyme was detected by staining with Coomassie brilliant blue R-250 for about 1 hour. The gel was then allowed to destain in methanol/glacial acetic acid solution overnight for visualization of the bands. The identity of the holoenzyme was confirmed by co-electrophoresed high molecular weight protein standards (GE Healthcare, Buckinghamshire, UK).

Western Blot

The ability of the mutant enzymes to properly assemble into a holoenzyme was screened by western blotting of nondenaturing gels containing extracts (10 µg/lane) from the cultures. Protein concentration was determined using the CB-X protein assay (G-Biosciences, St. Louis, MO). The SDS gel was electroblotted to PVDF. The Western Blot was run at a constant 200 mA for 30 minutes. The membrane was then removed and was soaked in Ponceau S staining solution (0.1% Ponceau S, 5.0% acetic acid; Sigma-Aldrich, St. Louis, MO) to verify that transfer was successful and to mark the standards with a pencil. The membrane failed to destain in .2 mM NaOH 20% acetonitrile but was instead destained in 5% acetic acid with methanol overnight with shaking. The following day, the methanol and acetic acid was removed and the gel was washed 3 times for 10 minutes with 1X Phosphate buffered saline(1.4 mM KH_2PO_4, 8 mM Na_2HPO_4, 140 mM NaCl, 2.7 mM KCl) with 0.05% Tween-20

(Sigma-Aldrich, St. Louis, MO). It was after this step that the pink color from the Ponceau S actually destained. The primary antibody (polyclonal rabbit anti-RubisCO) was then applied for about 3 hours. After three more washes with PBS-Tween, 50 ml of 1:100000 of donkey anti-rabbit HRP conjugate (secondary antibody) was added and left on for approximately 2.5 hours. The membrane was then washed again with PBS-Tween and incubated in a working detection solution provided with the OptiBlaze West femtoLUCENT kit (G-Biosciences, St. Louis, MO) for 3-5 minutes at room temperature with gentle shaking. The detection reagent was then drained and the membrane was placed in a plastic sleeve and exposed by chemiluminescence to an autoradiography film using a Fuji LAS 3000 (FujiFilm Medical Systems, Stamford, CT).

Molecular Modeling

All molecular files were downloaded from the Protein Data Bank. In some cases, the PDB files (PDB accession number 1RBL) for particular molecules were modified using Deep View software version 3.7b2 (Guex and Peitsch, 1997), or created *de novo* using Deep View, to construct the RubisCO enzyme from *Synechococcus PCC6301*.

RESULTS

Site-directed mutagenesis

Site-directed mutagenesis was performed to examine the functional significance of residue 47. To determine this significance, Alanine-47 of the large subunit gene was mutated to glycine or proline as described under "Materials and Methods". The target plasmid, pBGL710, was subjected to mutagenesis and the A47G and A47P mutants were identified by complete DNA sequencing and no additional mutations were found.

Effect of mutations on carboxylase activity

After the A47P and A47G mutants were verified through sequencing, further studies were carried out to measure the carboxylase activity. Cultures were grown for 3 hours and then induced with 0.5 mM IPTG for 8 h. The OD_{595} was measured at the time of induction. It should be noted that in all experiments, the OD of the wild-type was always higher than the mutants after three hours of growth (before induction). The activity of RubisCO from cultures of *E. coli* expressing each of the mutant enzymes was determined after permeabilization of the cells with CTAB or by

sonication. For calculation of specific activity, protein concentration was estimated using the Lowry Method for whole cells and the Bradford Method for extracts as described above. Whole cells were assayed along with extracts as a backup since enzymes can become denatured or inactivated during the sonication process.

Both of the mutant enzymes showed different levels of carboxylase activity with neither mutant showing a higher level of specific activity than the wild-type (Table 5 and Table 6). While absolute levels of specific activity differs between whole cells and extracts, the relative change is similar for each type of mutation.

Table 5. Average RubisCO activity, with standard deviations, in *E. coli* crude extracts for 10 quadruplicate trials.

RubisCO expressed	Specific Activity[a]	Relative Activity
	8 h induction[b]	
wild type	283±107	
A47G	33±14	12%
A47P	119±34	42%

[a]Expressed as nmol CO_2 fixed/min/mg protein in the crude extract. In each trial, a student's t-test support that the mutants and wild-type differed significantly, with p-values <.05.
[b]With a 1% inoculum from an overnight culture, cultures were grown for 3 hours and then induced with IPTG to 0.5 mM. They were harvested 8 hours after induction.

Table 6. Average RubisCO activity, with standard deviations, in *E. coli* whole cells for 10 quadruplicate trials.

RubisCO expressed	Specific Activity[a]	Relative Activity
	8 h induction[b]	
wild type	152±63	
A47G	21±13	14%
A47P	79±39	52%

[a]Expressed as nmol CO_2 fixed/min/mg protein in the crude extract. In each trial, a student's t-test support that the mutants and wild-type differed significantly, with p-values <.05.
[b]With a 1% inoculum from an overnight culture, cultures were grown for 3 hours and then induced with IPTG to 0.5 mM. They were harvested 8 hours after induction.

Assembly and enzymology of RubisCO

To examine the possibility that the decrease in specific activity was due to low expression or poor assembly of the mutant enzymes, SDS-PAGE, native-PAGE and Western Blots were performed. For all protein gels, the Bradford Assay was used to estimate protein concentration. The Bradford Assay was selected over the Lowry Assay simply to save time. Samples of each mutant were electrophoresed in the presence (Fig. 7) and absence (Fig. 8) of SDS. In the presence of SDS, large subunits of expected size were generated in all samples. Additionally, there was a

doublet band present in the mutants (lanes 4-8) that was not present in the wild-type (lanes 2 and 3). Both of the mutants expressed various amounts of RubisCO, but neither had a higher level of subunits than the wild-type.

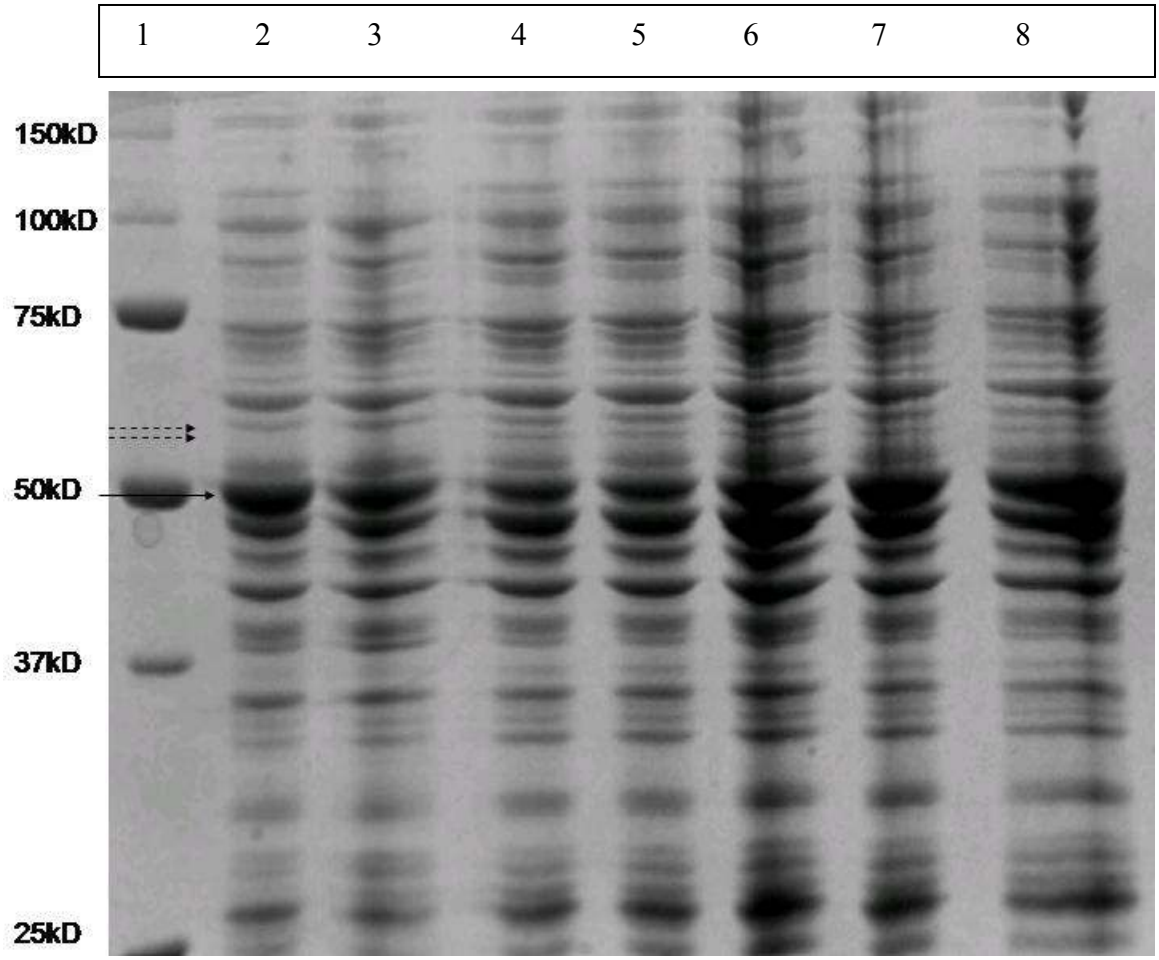

Lane	2	3	4	5	6	7	8
Sample	WT +IPTG	WT -IPTG	G Replicate 1	G Replicate 2	G Replicate 3	P Replicate 1	P Replicate 2
Specific activity	277	193	30	33	36	149	119

Figure 7. Coomassie-stained SDS polyacrylamide gel of wild type and mutants of whole cells. To each lane, 10 µg of protein was added. A solid arrow indicates the band corresponding to the LSU. A doublet that is present in the mutants but not present in the wild-type is indicated by dotted arrows.

Nondenaturing gel electrophoresis was performed in 6% polyacrylamide gels with *E. coli* crude extracts containing mutant enzymes. Nondenaturing gels allow the user to

resolve samples while retaining structure. Electrophoresis under nondenaturing conditions shows that the P mutant ran in a similar position (550 kDa) to the wild-type enzyme indicating that the A47P substitution in the large subunit had little or no effect on assembly of the L_8S_8 complex. However, the G mutant showed only a faint band at the same position.

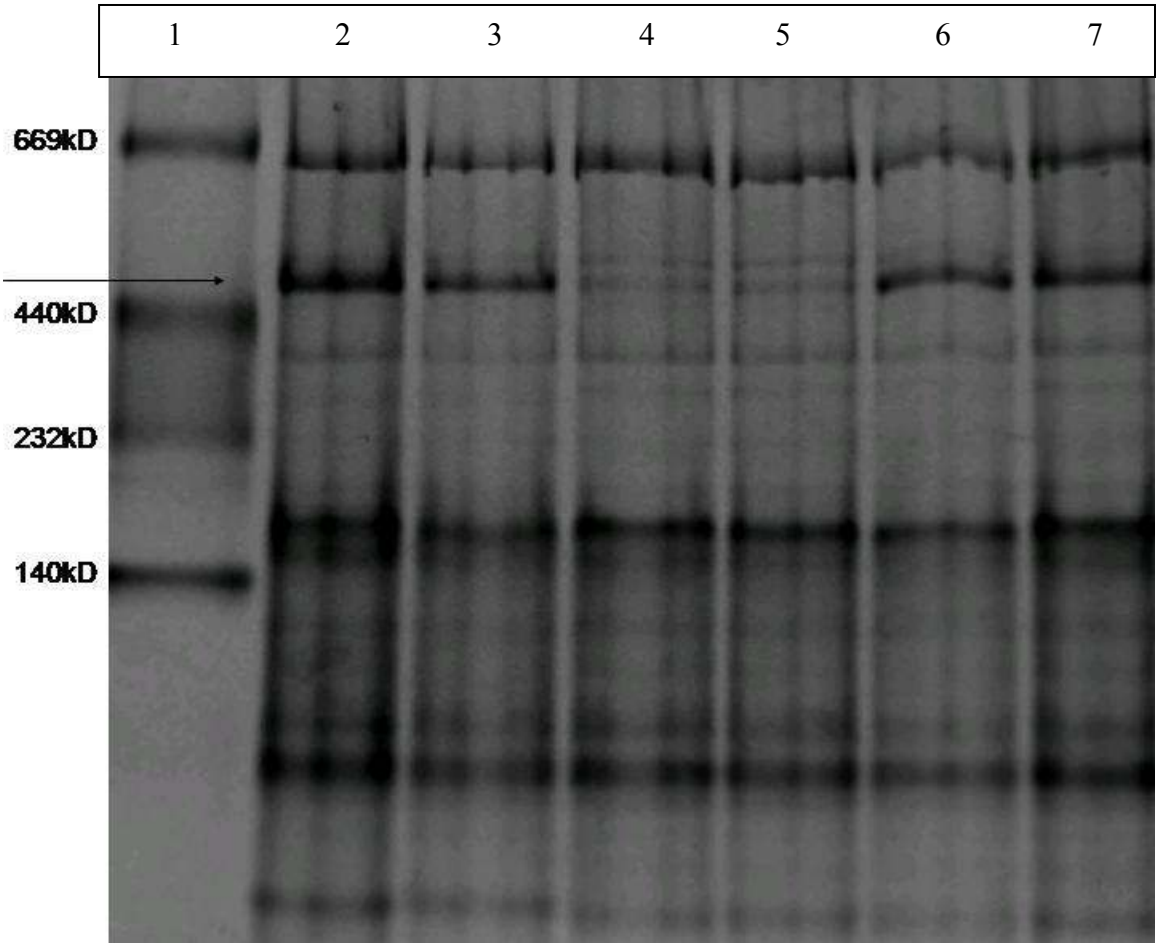

Lane	2	3	4	5	6	7
Sample	WT +IPTG	WT -IPTG	G Replicate 1	G Replicate 2	P Replicate 1	P Replicate 2
Specific activity	285	253	37	39	141	126

Figure 8. Coomassie stained non-denaturing gel of wild type and mutants of extracts. PAGE was performed in 6% acrylamide gels with 10 µg of each extract using the Laemelli gel system in the absence of SDS. Lane 1, HMW marker; Lane 2, pBGL710 induced; Lane 3, pBGL710 uninduced; Lane 4, A47G replicate 1; Lane 5, A47G replicate 2; Lane 6, A47P replicate 1; Lane 7, A47P replicate 2. The molecular weight standards were thyroglobulin (669kD), ferritin (440kD), catalase (232kD), lactate dehydrogenase (140kD), and bovine serum albumin (67kD). An arrow indicates the band corresponding to the RubisCO holoenzyme (L8S8).

E. coli extracts were also used for Western Blotting (Figure 9) of denaturing polyacrylamide gels to confirmed that the band that was being called RubisCO in the above gels is actually RubisCO and that normal amounts of protein were present (with the exception of the G mutant). Since the P mutant had comparable amounts of protein present, some property of the mutant enzyme may have resulted in the difference in specific activities.

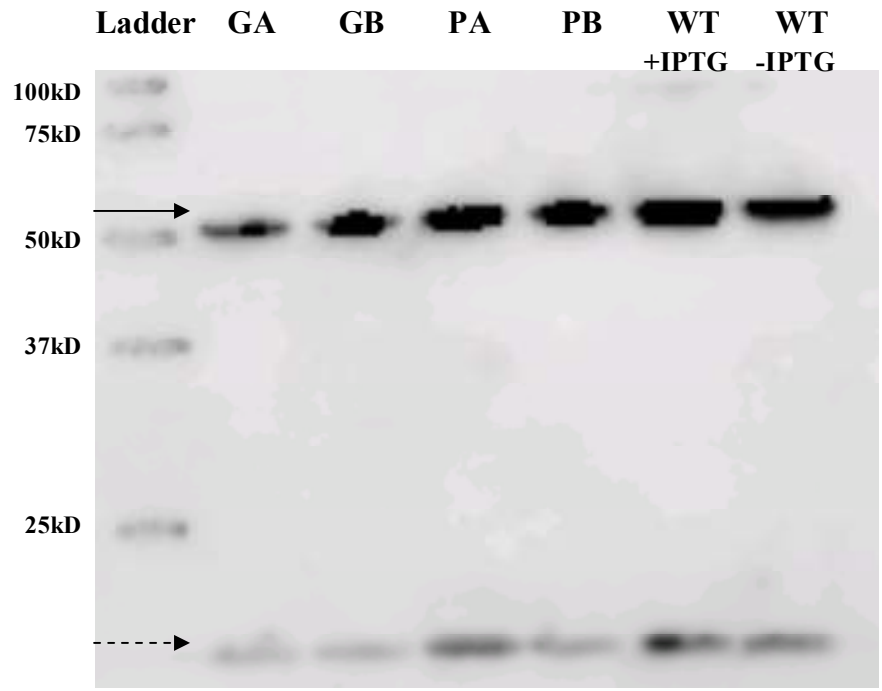

Figure 9. Western Blot analysis of total subunit proteins. Extracts (10 µg/lane) were fractionated by SDS-polyacrylamide gradient (10%) gel electrophoresis. Proteins were blotted to nitrocellulose, probed with anti-RubisCO immunoglobulin G (0.5 µg /ml), and detected by chemiluminescence. A solid arrow indicates the band corresponding to the LSU. The dotted arrow indicates the band corresponding to the SSU.

To examine the effect of mutating Alanine 47, a model of residues 35-70 of the LSU from Synechococcus PCC6301 were constructed *in silico*. Comparison of both mutants to the wild-type reveal significant differences when compared (Figure 10). Molecular modeling shows a strong hydrogen

bond (indicated in green) between residues A47 and Glycine-54 in the wild type, as well as the weak hydrogen bond (indicated in gray) between residues A47 and Alanine-43 in the wild-type. These bonds are also present in the P mutant but are both absent in the G mutant.

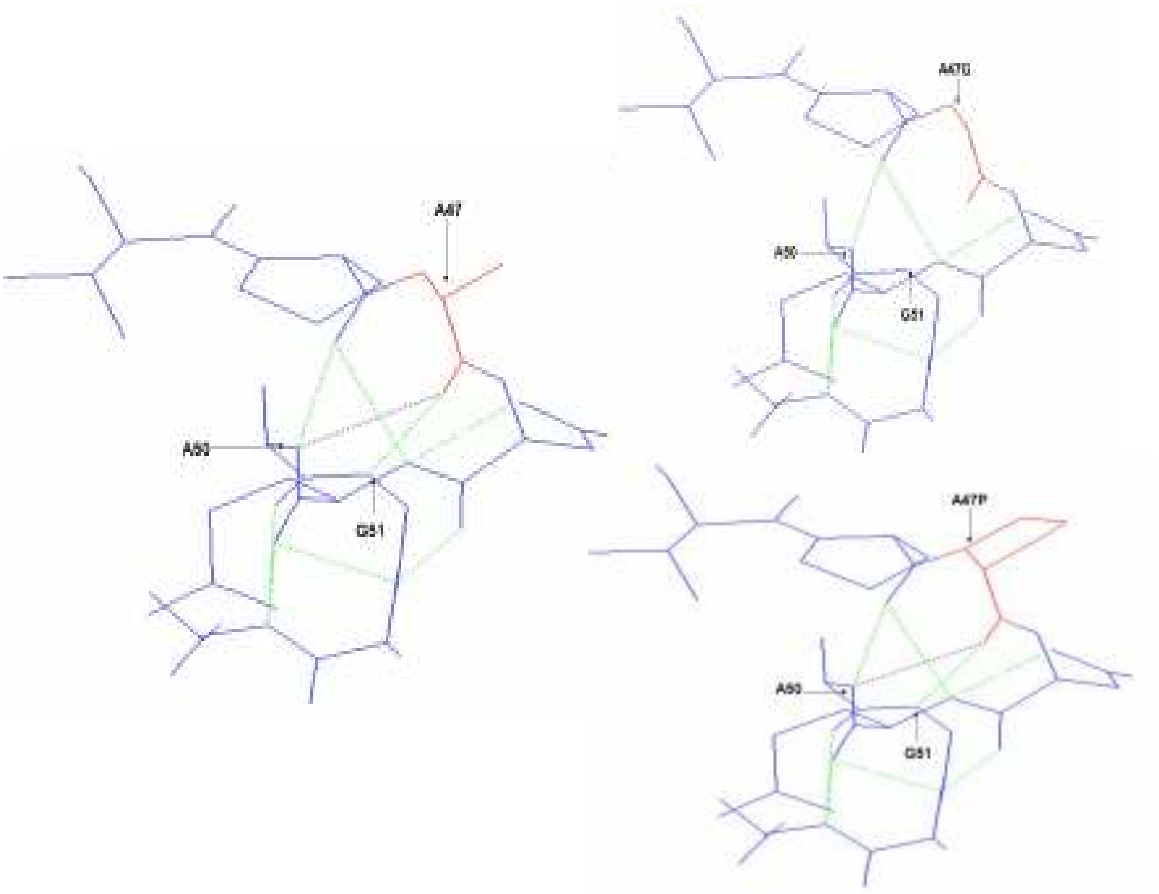

Figure 10. In silico modeling of residues 45-53 in the mutants and wild-type. All models were created using DeepView in the Swiss Protein Database Viewer, version 3.7b2. In all models, the wild-type or mutant residue at position 47 is shown in red. Strong hydrogen bonds are in green whereas weak hydrogen bonds are in black.

DISCUSSION

Since RubisCO is the enzyme that catalyzes the rate-limiting step of photosynthesis but has a carboxylation rate of 2-3 molecules per second, and is competitively inhibited by molecular oxygen, it is an obvious target for genetic engineering with the hopes of increasing primary productivity in crop plants.

Alanine-47 plays a critical role in *Synechococcus PCC6301* RubisCO since both A47P and A47G resulted in a decrease in specific activity relative to the wild-type. Substitutions at Alanine 47 are detrimental to carboxylation. In crude extracts in *E. coli*, the P mutant had 42% specific activity relative to the wild-type enzyme whereas the G mutant had 12% activity relative to the wild-type (Table 5). In whole cells in *E. coli*, the P mutant had 52% specific activity relative to the wild-type whereas the G mutant had a 14% activity relative to the wild-type (Table 6). The higher specific activity in whole-cells in the P mutant when compared to the extracts might be due to RubisCO being in a more favorable conformation in the whole cell. This result is not what was hypothesized especially

since alanine and glycine share many similar properties. Both amino acids have a neutral charge, have similar molecular weights, and have aliphatic R-groups.

Since the G mutant resulted in such low specific activity, it was hypothesized that the enzyme was not being expressed properly. SDS-PAGE was performed to determine whether the specific activity correlated with the expression of the enzyme. SDS-PAGE was inconclusive in terms of expression. SDS-PAGE indicated that there were approximately equal amounts of large subunit polypeptide present for all samples (Figure 7). A Western Blot was performed for better qualitative assessment.

Since the G mutant resulted in such low activity, it was hypothesized that the enzyme would not be able to assemble properly. This hypothesis is based on the fact that analysis of the Rubisco holoenzyme through molecular modeling (Figure 10) indicated that this mutation would remove significant structural elements, such as hydrogen bonding, that could affect holoenzyme assembly. The strong hydrogen bond (indicated in green) between residues 47 and Glycine-51 in the wild type, as well as the weak hydrogen bond (indicated in gray) between residues 47 and Alanine-40, still remained in mutant A47P. When residue 47 was

changed to a glycine residue in the model, both of these hydrogen bonds disappeared. Perhaps, this extra rigidity from this common hydrogen bond in the wild-type and P mutant might be responsible for their higher specific activities.

In general (ignoring specific tertiary interactions), the mutation of an alanine residue on the surface of a protein to a proline will tend to stabilize the folded state whereas a mutation to a glycine will tend to destabilize the folded state (Richardson, 1981). This is because proline has a restricted conformation space whereas glycine has a large conformation space. Proline lacks the normal backbone N-H for hydrogen bonding. Proline has been show to force structural elements to turn at the surface, so that in spite of its hydrophobicity, it is usually found near the protein surface (Richardson, 1981). Since glycine's unique sidechain is only a hydrogen and is much less "sterically disadvantaged", it can assume conformations normally restricted by close contacts of the beta-carbon and is more flexible than other residues, thus contributing to parts of the backbone that need to move or hinge (Richardson, 1981). Furthermore, proline can bend the polypeptide on itself, making the backbone more open to

hydrogen bonding with the polar side chains of other turn formers (Levitt, 1978; Lewis *et al.*, 1973). Contrastingly, proline is not very common in helices due to steric hindrance arising from its cyclic sidechain that blocks the main chain NH group (Hurley et al., 1992). However, when Proline does occur in an alpha-helix, it is usually located in the first turn acting as an N-capping residue (Richardson and Richardson, 1988). Perhaps, it is for this reason that Proline is highly conserved at residue 47 (at the beginning of a helix) across RubisCOs.

Therefore, the substitutions of Alanine 47 for a glycine might cause major disruption to the tertiary structure of the large subunit. Furthermore, the intricacy and the size of RubisCO, an enzyme with a molecular mass of about 550 kDa made up of 16 subunits from two gene products, would further complicate the synthesis and assembly of an active enzyme. Native PAGE demonstrates that the mutant enzymes are defective in holoenzyme assembly. In particular, there appears to be significantly less protein in the G mutant lanes on the gel (Figure 8, lanes 4 and 5). Perhaps the G mutant is a folding-mutant since Glycine does not have any detectable holoenzyme on nondenaturing PAGE (Figure 8, lanes 4 and 5). In addition,

holoenzyme assembly may have been prevented in the G mutant by interfering with a reaction between the *E. coli* GroEL with the large and small subunits. GroEL is a protein chaperone that is required for the proper folding in many proteins in prokaryotes. The *E. coli* GroEL gene product is required for assembly of cyanobacterial RubisCO in *E. coli* (Goloubinoff et al., 1989).

Western Blots of denaturing gels were performed to confirm that the bands that were being called the LSU in the SDS-PAGE gels were actually the RubisCO large subunit and to qualitatively assess the expression levels of that protein (Figure 9). Western Blotting confirmed that the bands being called RubisCO were indeed RubisCO. Since the P mutant had comparable amounts of protein present, some property of the mutant enzyme may have resulted in the difference in specific activities.

As with all enzyme assays, there was much potential room for error. For all cell culture experiments, the OD was measured at the time of induction (after three hours) at 595 nm. Originally, the cells were going to be cultivated until an OD of 0.3 (early-mid log phase) for IPTG-induction but after three hours of growth, the OD varied dramatically between the mutants and the wild-type. Further studies should be done to determine if growing the

mutants to an OD of 0.3 prior to induction would change the specific activity.

Additionally, the bacterial strain that the mutants and wild-type were grown in were different. The mutants were created using the site-directed mutagenesis kit from Stratagene. The mutant DNA was transformed into *E. coli* XL1-Blue [*recA1 endA1 gyrA96 thi-1 hsdR17 supE44 relA1 lac* [F′::Tn*10* (Tet^{r}) *proAB* Δ*lacI*^{q} *(lacZ)M15*]] competent cells. The wild-type, pBGL710, was transformed into JM109 [e14- (McrA-) *recA1 endA1 gyrA96 thi-1 hsdR17* (*r*K - *m*K +) *supE44 relA1* Δ(*lac-proAB*) [F´ *traD36 proAB lacI*q*Z*Δ*M15*]]. Stratagene lists XL1-Blue's genotype as identical to E. coli JM109 (except the F'). However, working with both strains has made it obvious that there must be some fundamental difference between them. XL1 grows significantly slower than JM109. The use of two different bacterial strains in this study most probably explains the dramatic difference in OD between the mutants and wild-type at the time of induction. The mutant plasmids should have been transformed into JM109 for accurate comparison with the wild-type. To investigate if the mutants would behave in a similar manner when transformed into JM109, a follow-up experiment was later performed as described in Appendix B.

If this study were to be carried out further, RubisCO should be purified in order to investigate the kinetic properties of the mutant enzymes. This is particularly important for the P mutant, since the G mutant did not form a holoenzyme. These properties include the specificity, k_{cat}, and affinity for CO_2. In addition, attempts to isolate second-site suppressors would enable us to gain insights into how to stabilize the core domain of the mutants and ultimately engineer an improved enzyme. A second-site suppressor is a second-site mutation that, in the presence of the original mutation, modifies the original phenotype of the strain to be enough like that of wild-type. Finding second-site suppressors would allow us to identify other complementing regions of the enzyme. Perhaps, second-site suppressors could be made with residues 43 and 54 in which molecular modeling in this experiment has shown to interact with Alanine-47.

Furthermore, to further confirm that the A47P mutant does not affect the structural stability of RubisCO, thermal stability experiments could be performed. I would hypothesize that the P mutation would not affect thermal stability since others have demonstrated that proline residues are important for thermal stability (Matthews et al., 1987). It would be interesting to see if the P mutant

is stable since the activity of an enzyme can be reduced by the extent of thermal denaturation. Perhaps the principle route(s) of degradation could be identified by subjecting the protein to increased temperatures.

The results presented here indicate that Alanine 47 is a critical residue in Synechococcus RubisCO. Perhaps the greatest significance of this study is the demonstration that a conservative mutation at residue 47 can have dramatic effects on holoenzyme assembly. Furthermore, the substitution A47G is shown to disrupt a network of hydrogen bonds, which may explain the reduced specific activity in this mutant. Considering how mutations at A47 can influence holoenzyme assembly, further studies of residues distal from the active site may provide clues for engineering an improved enzyme. This work, along with other RubisCO mutant studies, demonstrate how mutations remote from the active site can play a significant role in the stability and function of RubisCO and can be manipulated to modify catalytic function. The simultaneous mutation of multiple residues far from the active-site may even be required to improve RubisCO efficiency (Andrews and Whitney, 2003). However, genetic selection for a better enzyme may not be feasible if more than a few amino acids need to be manipulated. Because of RubisCO's role in plant

productivity and controlling global warming, further study of this enzyme is necessary.

Appendix A

Mutant plasmids were removed from the -20°C freezer as described above in the materials and methods. Mutants A47P and A47G were transformed into *E. coli* JM109, which was grown in LB medium. To maintain selective conditions for the mutants, the agar and liquid media contained 50 µg/ml of ampicillin. Following transformation and incubation, the plates were streaked for isolation on LB-amp plates. 2 ml overnight cultures were prepared in duplicate as previously described. 1 ml of the overnight culture was to be used for growth and induction while the remaining ml was used to make glyercol stocks of the transformed mutants. For expression of RubisCO genes, 100 mM isopropyl B-D-thiogalactopyranoside was added to a final concentration of 0.5 mM IPTG after 3 hours of growth. After induction, cultures were incubated at 37°C with shaking for 8 hours prior to harvesting. To determine the specific activity of the mutants and wild-type, total protein concentration was calculated using a modification of the Lowry Method as described above. A RubisCO assay and SDS-PAGE gel were performed as described previously. Following the RubisCO

assay and SDS-PAGE gel, the samples were placed back in the -20°C freezer and subjected to an additional freeze-thaw cycle prior to PAGE analysis.

With Mutants in JM109		With Mutants in XL1-Blue	
Sample	**OD_{595}**	**Sample**	**OD_{595}**
GA	0.232	GA	0.042
GB	0.237	GB	0.038
GC	0.185	GC	0.042
GD	0.165	GD	0.053
WTA	0.129	WTA	0.136
WTB	0.143	WTB	0.122
WTC	0.144	WTC	0.123
WTD	0.140	WTD	0.111
PA	0.194	PA	0.070
PB	0.212	PB	0.060
PC	0.185	PC	0.053
PD	0.189	PD	0.046

Table A1. Comparison of Optical Densities in XL1-Blue and JM109. The OD at the time of induction was measured at 595 nm using a Milton Roy Spectronic 401 (Milton Roy, Ivyland, PA). The mutants demonstrated more than a 3-fold increase in OD in JM109. After induction, cultures were incubated at 37C with shaking for 8 hours prior to harvesting.

Table A2. Average RubisCO activity, with standard deviations, in JM109 crude extracts for 1 quadruplicate trial.

RubisCO expressed	Specific Activity[a]	Relative Activity
	8 h induction[b]	
wild type	55±17	
A47G	16±5	29%
A47P	37±3	68%

[a]Expressed as nmol CO_2 fixed/min/mg protein in the crude extract. For this trial, a student's t-test support that the mutants and wild-type differed significantly, with p-values <.05.
[b]With a 1% inoculum from an overnight culture, cultures were grown for 3 hours to an approximate OD of 0.200 and then induced with IPTG to 0.5 mM. Cultures were harvested 8 hours after induction.

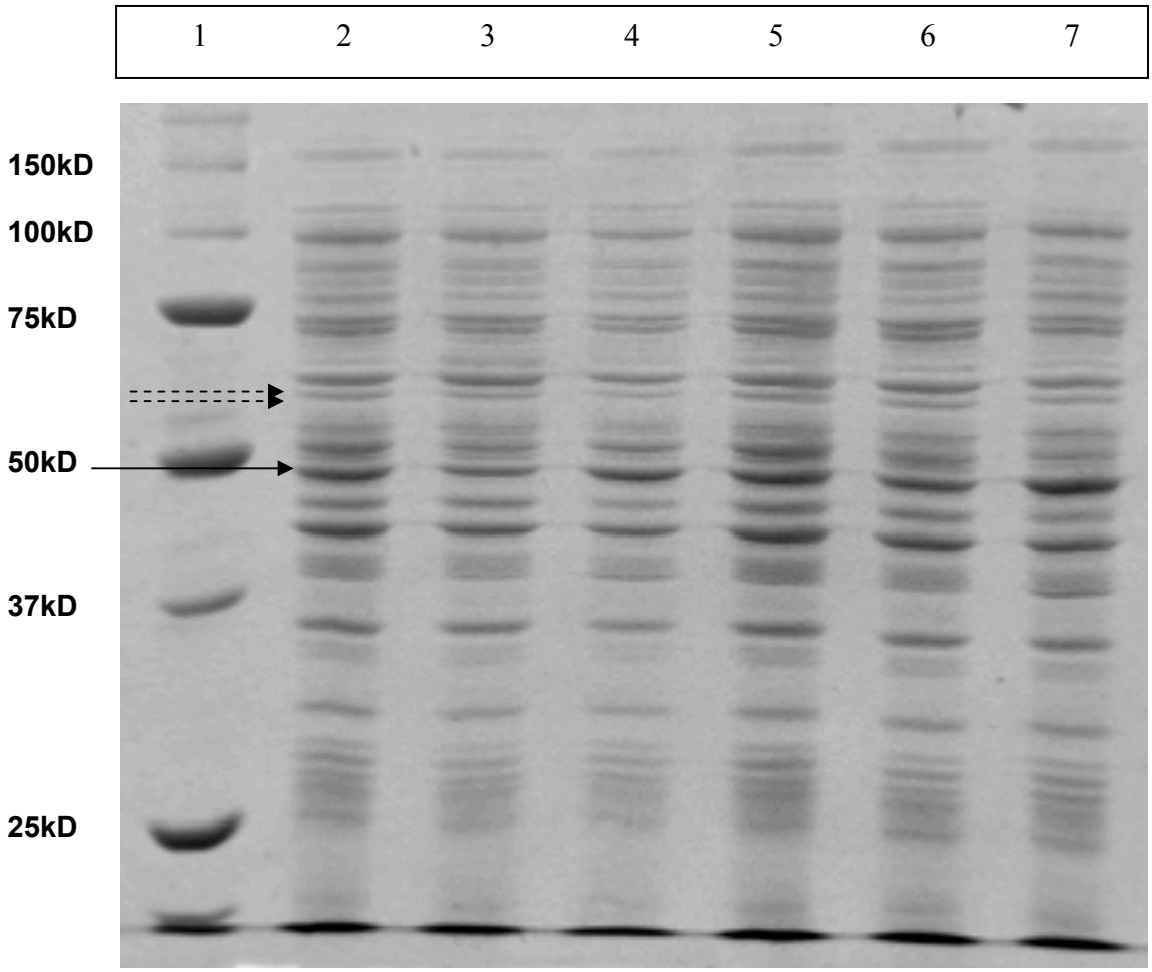

Lane	2	3	4	5	6	7
Sample	P Replicate 1	G Replicate 1	WT +IPTG	P Replicate 2	G Replicate 2	WT -IPTG
Specific activity	36	21	48	38	11	7

Figure A1. Coomassie-stained polyacrylamide gel of wild type and mutants of extracts. To each lane, 10 µg of protein was added. A solid arrow indicates the band corresponding to the LSU. Dotted arrows indicate where the doublet band was present in the XL1-Blue mutants.

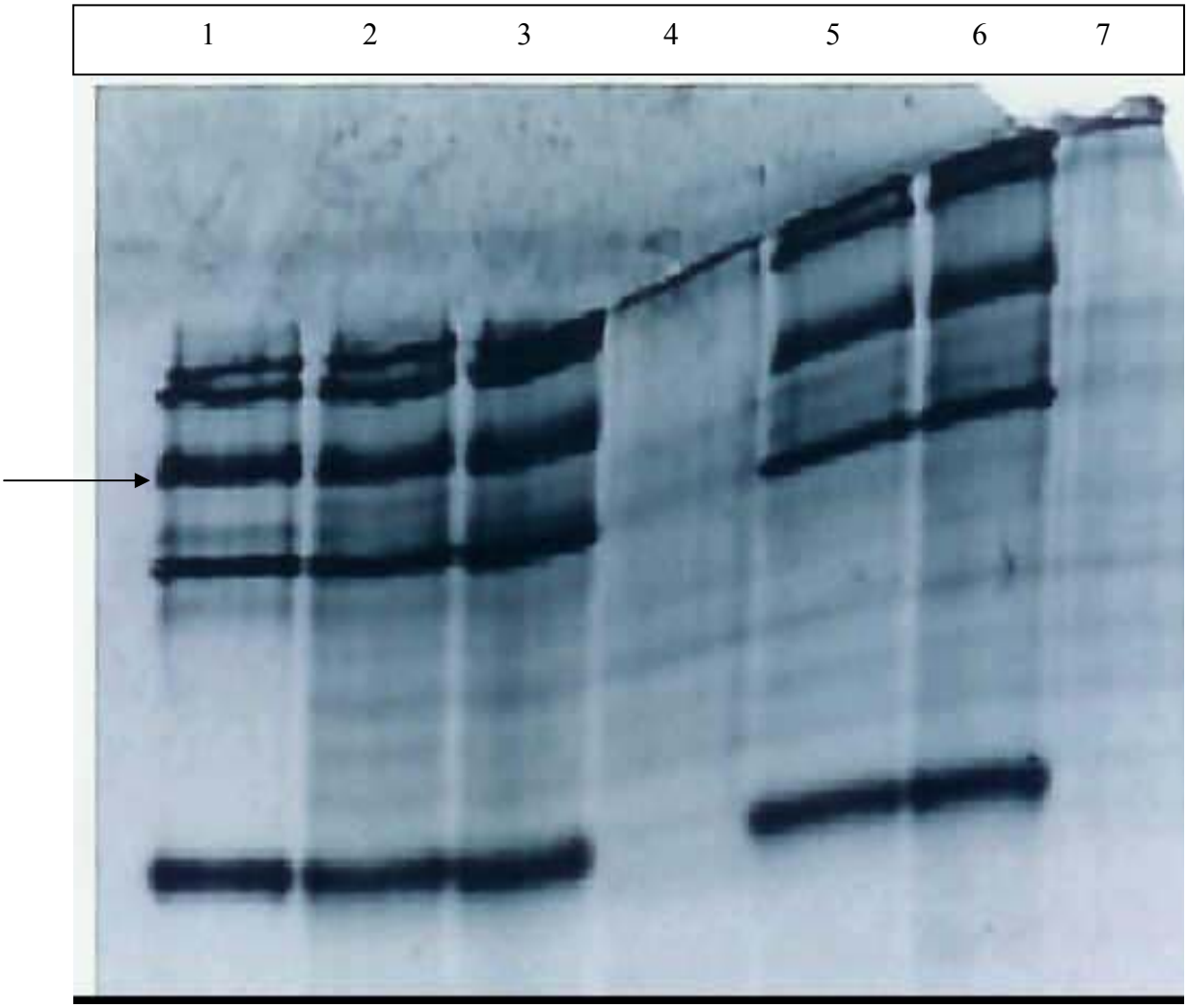

Lane	2	3	4	5	6	7
Sample	WT +IPTG	P Replicate 1	G Replicate 2	WT -IPTG	P Replicate 2	G Replicate 2
Specific activity	48	36	21	7	38	11

Figure A2. Coomassie stained non-denaturing gel of wild type and mutants of extracts. PAGE was performed in 6% acrylamide gels with 10 µg of each extract using the Laemelli gel system in the absence of SDS. Lane 1, HMW marker; Lane 2, pBGL710 induced; Lane 3, A47P; Lane 4, A47G; Lane 5, pBGL710 uninduced; Lane 6, A47P; Lane 7, A47G. The molecular weight standards were thyroglobulin (669kD), ferritin (440kD), catalase (232kD), lactate dehydrogenase (140kD), and bovine serum albumin (67kD). An arrow indicates the band corresponding to the RubisCO holoenzyme (L8S8).

Discussion

In crude extracts in *E. coli*, the P mutant had 68% specific activity relative to the wild-type enzyme whereas the G mutant had 30% activity relative to the wild-type (Table A2). The lower specific activities might be due the IPTG stock being degraded in the freezer or made at the incorrect concentration. When induced previously at 0.5 mM IPTG, the wild-type specific activity was 283 (Table 5). In this experiment, the specific activity for the wild-type was 48 which would be expected if the cells were induced at 0.1 M IPTG. Induction temperature and shaking speed during culturing were the same for each experiment as induction temperature and shaking speed can influence specific activity.

SDS Page indicated that there was slightly less of the large subunit polypeptide present for the mutants, especially the A47G mutant (Figure A1). It should also be noted that the doublet band that was present in Figure 7, is not present in the mutants in this gel. This should be a clear indication that the doublet that was seen in the

previous gel was due to the mutants being in a different strain of E. coli than the wild-type.

It is inconclusive from this Native PAGE gel that the G mutant is defective in holoenzyme assembly. There appears to be significantly less protein in the G mutant lanes on the gel (Figure A2, lanes 4 and 7). Since the G mutant underwent two freeze-thaw cycles and already had reduced specific activity and structural stability, the reduction in protein might be due to degradation from multiple freeze-thawing. The P mutant however was still able to form a holoenzyme that is comparable to the wild-type. The High Molecular Weight ladder that was loaded in lane 1 looks similar to lane 2 most probably due to spill-over during loading. Also, it should be noted that when the resolving gel was poured, it wasn't completely linear when it polymerized. This is what gives this figure the "crooked" appearance.

It can be concluded that mutants A47G and A47P behave in a similar manner in JM109 as in XL1-Blue. Both mutants demonstrated lower specific activity, and showed less expression than the wild-type as previously shown in XL1-Blue. Additionally, the G mutant was defective for holoenzyme assembly in JM109 as it was previously defective in XL1-Blue although this may be explained by multiple

freeze-thaw cycles. Although this trial was performed in quadruplicate, further trials should be performed to validate that this conclusion holds true.

References

Andersson, I., Knight, S., Schneider, G., Lindqvist, Y., Lindqvst, T, Branden, C.I., and Lorimer, G.H. (1989) Crystal structure of the active site of ribulose-1,5-bisphosphate carboxylase. *Nature* **337**:229–234

Andersson I. (1996) Large structures at high resolution: the 1.6 angstrom crystal structure of spinach ribulose-1,5-bisphosphate carboxylase/oxygenase complexed with 2-carboxyarabinitol bisphosphate. *J. Mol. Biol.* **259**:160–174.

Andersson, I., and Taylor, T.C. (2003) Structural framework for catalysis and regulation in ribulose-1,5-bisphosphate carboxylase/oxygenase. *Arch. Biochem. Biophys.* **414**:130-140.

Andrews, T.J., and Ballment, B. (1983) The function of the small subunits of ribulose bisphosphate carboxylase-oxygenase. *J. Biol. Chem.* **258**:7514–7518.

Andrews, T.J., and Whitney, S.M. (2003) Manipulating ribulose bisphosphate carboxylase/oxygenase in the chloroplasts of higher plants. *Arch. Biochem. Biophys*. **414**:159-169.

Andrews, T.J., Lorimer, G.H., and Tolbert, N.E. (1971) Incorporation of molecular oxygen into glycine and serine during photorespiration in spinach leaves. *Biochemistry* **10**:4777–4782.

Bainbridge, G., Anralojc, P.J., Madgwick, P.J., Pitts, J.E., and Parry, M.A.J. (1998) Effect of mutation of lysine-128 of the large subunit of ribulose bisphosphate carboxylase/oxygenase from *Anacystis nidulans*. *Biochem.* **336**:387-393.

Berman, H.M., Westbrook, J., Feng, Z., Gilliland, G., and Bat, T.N. (2000) The Protein Data Bank. *Nuc. Acids Res.* **28**:235-242.

Bowes, G., and Ogren, W.L. (1970) The effect of light intensity and atmosphere on ribulose diphosphate carboxylase activity. *Plant Physiol.* (Suppl) **46**:7.

Bradford, M.M. (1976) A rapid and sensitive method for the quantitation of microgram principle of protein dye binding. *Anal. Biochem.* **72**:248-254.

Chapman, M.S., Won Suh, S., Currie, P.M.G., Cascio, D., Smith, W.W., Eisenberg, D. (1988) Tertiary structure

of plant Rubisco: domains and their contacts. *Science* **241**:71-74.

Chen, Z., and Spreitzer, R.J. (1992) How various factors influence the CO_2/O_2 specificity of ribulose-1,5-bisphosphate carboxylase/oxygenase. *Photosynthesis* **31**:157-164.

Ehleringer, J.R., Sage, R.F., Flanagan, L.B., and Pearcy, R.W. (1991) Climate change and the evolution of C4 photosynthesis. *Trends in Ecology and Evolution* **6**:95-99.

Ellis, R.J. (1979) The most abundant protein in the world. *Trends Biochem. Sci.* **4**:241-244.

Farquhar, G.D., von Caemmerer, S., and Berry, J.A. (1980) A biochemical model of photosynthetic CO2 assimilation in leaves of C3 plants. *Planta* **149**:78-90.

Goloubinoff, P., Gatenby, A.A., and Lorimer, G.H. 1989 GroE heat-shock proteins promote assembly of foreign prokaryotic ribulose bisphosphate carboxylase oligomers in Escherichia coli. *Nature (London)* **337**:44-47.

Guex, N., and M.C. Peitsch. (1997) SWISS-MODEL and the Swiss-PdbViewer: an environment for comparative protein modeling. *Electrophoresis* **18**:2714-2723.

Gutteridge, S., Millard, B.N., and Parry, M.A.J. (1986) *FEBS Lett.* **196**:263-268.

Hansen, S., Vollan, V.B., Hough, E., and Andersen, K. (1999) The crystal structure of rubisco from Alcaligenes eutrophus reveals a novel central eight-stranded β-barrel formed by β-strands from four subunits. *J. Mol. Biol.* **288**:609-621.

Hanson, E., and Tabita, R. (2001) A ribulose-1,5-bisphosphate carboxylase/oxygenase (RubisCO)-like protein from *Chlorobium tepidium* that is involved with sulfur metabolism and the response to oxidative stress. *Proceedings of the National Academy of Sciences*. **98**:4397-4402.

Hartman, F.C., and Harpel, M.R. (1994) Structure, function, regulation and assembly of ribulose-1,5-bisphosphate carboxylase/oxygenase. *Annu. Rev. Biochem.* **63**:157-234.

Hernandez, J.M., Baker, S.H., Lorbach, S.C., Shively, J.M., and Tabita, F.R. 1996 Deduced amino acid sequence, functional expression, and unique enzymatic properties of the form I and form II ribulose bisphosphate carboxylase/oxygenase from the chemoautotrophic bacterium *Thiobacillus denitrificans*. *J. Bacteriol.* **178**:347-356.

Horken, K.M., and Tabita, F.R. (1999) The "green" form I riblose 1,5-bisphosphate carboxylase/oxygenase from the nonsulfur purple bacterium Rhodobacter capsulatus. *J. Bacteriol.* **181**:3935-3941.

Houtz, R.L., Stults, J.T., Mulligan, R.M., and Tolbert, N.E. (1989) Post-Translational Modifications in the Large Subunit of Ribulose Bisphosphate Carboxylase/Oxygenase. *Proc. Natl. Acad. Sci.* **86**:1855-59.

Hurley, J.H., Mason, D.A., and Matthews, B.W. (1992) Flexible-geometry conformational energy maps for the amino acid residue preceding a proline. *Biopolymers* **32**:1443-1556.

Igarashi, Y., and Kodama, T. (1996) Genes related to carbon dioxide fixation in *Hydrogenovibrio marinus* and *Pseudomonas hydrogenothermophila*. In: Lidstrom ME and Tabita FR (eds) Microbial Growth on C1 Compounds, pp 88–93. Kluwer Academic Publishers, Dordrecht, The Netherlands.

Javadpour, M.M., Eilers, M., Groesbeek, M., and Smith, S.O. (1999) Helix packing in polytopic membrane proteins:role of glycine in transmembrane helix association. *Biophys J.* **77**:1609-1618.

Jordan, D.B., and Ogren, W.L. (1981) Species variation in the specificity of ribulose bisphosphate carboxylase/oxygenase. *Nature.* **291**:513-515.

Kaplan, A., and Reinhold, L. (1999) CO_2 concentrating mechanisms in photosynthetic microorganisms. *Annu. Rev. Plant Physiol. Plant Mol. Biol.* **50**:539-570.

Kellogg, E.A., and Juliano, N.D. (1997) The structure and function of RubisCO and their implications for systematic studies. *Am. J. of Bot.* **84**:413-428.

Laemmli, U.K. (1970) Cleavage of structural proteins during the assembly of the head of bacteriophage T4. *Nature* **277**:680-685.

Larimer, F.W., and Soper, T.S. (1993) Overproduction of *Anabaena* 7120 ribulose-bisphosphate carboxylase/oxygenase in *Escherichia coli*. *Gene* **126**: 85–92.

Lee, G.J., McDonald, K.A., McFadden, B.A. (1993) Leucine 332 influences the CO_2/O_2 specificity factor of ribulose-1,5-bisphosphate carboxylase/oxygenase from *Anacystis nidulans*. *Protein Sci*. **2**:1147-1154.

Lee, B., and Tabita, F.R. (1990) Purification of recombinant ribulose-1,5-bisphosphate carboxylase/oxygenase large subunits for

reconstitution and assembly of active L_8S_8 enzyme. *Biochemistry* **29**:9352-9357.

Lee, B., and Tabita, F.R. (1991) Mutations in the small subunit of cyanobacterial ribulose-bisphosphate carboxylase/oxygenase that modulates interactions with small subunits. *J. Biol. Chem.* **266**:7417-7422.

Levitt, M. (1978) Conformational preferences of amino acids in globular proteins. *Biochemistry* **17**:4277–4284.

Lewis, P.N., Momany, F.A., and Scheraga, H.A. (1973) Chain reversals in proteins. *Biochim. Biophys. Acta.* **303**:211–229.

Li, H., Sawaya, M.R., Tabita, F.R., and Eisenberg, D. (2005) Crystal structure of a novel RuBisCO-like protein from the green sulfur bacterium *Chlorobium tepidum*. *Structure* 13:779-789.

Lorimer, G.H., Badger, M.R., and Andrews, T.J. (1976) The activation of ribulose-1,5-bisphosphate carboxylase by carbon dioxide and magnesium ions. Equilibria, kinetics, a suggested mechanism, and physiological implications. *Biochemistry*. **15**:529–536.

Lorimer, G.H., and Miziorko, H.M. (1980) Carbamate formation on the epsilon-amino group of a lysyl residue as the basis for the activation of ribulosebisphosphate carboxylase by CO_2 and Mg^{2+}. *Biochemistry* **19**:5321-5328.

Lowry, O.H., Rosbrough, N.J., Farr, A.L., and Randall, R.J. (1951) Protein measurement with the Folin Phenol reagent. *J. Biol. Chem.* **193**:265-275.

Maeda, N., Kitano, K., Fukui, T., Ezaki, S., Atomi, H., Miki, K., and Imanaka, T. (1999) Ribulose bisphosphate carboxylase/oxygenase from the hyperthermophilic archaeon *Pyrococcus kodakaraensis* KOD1 is composed solely of large subunits and forms a pentagonal structure. *J. Mol. Biol.* **293**:57-66.

Markwell, M., Haas, S.M., Bieber, L.L., and Tolbert, N.E. (1978) A modification of the Lowry method to simplify protein determination in membrane and lipoprotein samples. *Anal. Biochem.* **87**:206-210.

Matthews, B.W., Nicholson, H., and Becktel, W.J. (1987) Enhanced protein thermostability from site-directed mutations that decrease the entropy of unfolding. *Proc. Natl. Acad. Sci.* **84**:6663–6667.

Newman, J, and Gutteridge, S. (1993) The x-ray structure of Synechococcus ribulose-bisphosphate carboxylase/oxygenase-activated quaternary complex at 2.2-A resolution. *J. Biol. Chem.* **268**:25876-25886.

Pon, N.G., Rabin, B.R., and Calvin, M. (1963) Mechanism of the carboxydismutase reaction. *Biochem Z.* **338**:7-19.

Read, B.A., and Tabita, F.R. (1992) A hybrid ribulosebisphosphate carboxylase/oxygenase enzyme exhibiting a substantial increase in substrate specificity factor. *Biochemistry*. **31**:519-525.

Read, B.A. and Tabita, F.R. (1994) High substrate specificity factor ribulose bisphosphate carboxylase/oxygenase from eucaryotic marine algae and properties of recombinant cyanobacterial rubisco containing "algal" residue modifications. *Arch. of Biochem. and Biophys.* **312**(1):210-218.

Richardson, J.S. (1981) The anatomy and taxonomy of protein structures. *Adv. Protein Chem.* **34**:168-339.

Richardson, J.S., and Richardson, D.C. (1988) Amino acid preferences for specific locations at the ends of alpha helices. *Science* **240**: 1648-1652.

Satagopan, S., and Spreitzer, R.J. (2004) Substitutions at the Asp-473 latch residue of Chlamydomonas ribulosebisphosphate carboxylase/oxygenase cause decreases in carboxylation efficiency and CO_2/O_2 specificity. *J. Biol. Chem.* **279**:14240-14244.

Schneider, G., Lindqvist, Y., Branden, C.I., and Lorimer, G.H. (1986) Three dimensional structure of ribulose-1,5-bisphosphate carboxylase/oxygenase from *Rhodospirillum rubrum* at 2.9 Å resolution. *EMBO J.* **5**: 3409-3415.

Schneider, G., Lindqvist, Y., and Branden, C. (1992) Rubisco: Structure and Mechanism. Annu. Rev. Biophys. Biomol. Struct. **21**:119-143.

Smith, S.A. (2002) Design of a biological system to select for alterations in the key kinetic properties of ribulose 1, 5-bisphosphate carboxylase/oxygenase (RubisCO). Ph.D. Dissertation, The Ohio State University, Columbus, OH.

Smith, S.A., and Tabita, F.R. (2003) Positive and negative selection of mutant forms of prokaryotic (cyanobacterial) ribulose-1, 5-bisphosphate carboxylase/oxygenase. *J. Mol. Biol.* **331**:557-69.

Spreitzer, R.J., Brown, T., Chen, Z., Zhang, D., and Al-Abed, S.R. (1988) Missense Mutation in the Chlamydomonas Chloroplast Gene that Encodes the Rubisco Large Subunit. *Plant Physiol.* **86**:987-989.

Spreitzer, R.J., Salvucci, M.E. (2002) RubisCO: Structure, regulatory interactions, and possibilities for a better enzyme. *Annu. Rev. Plant Physiol. Plant Mol. Biol.* **53**:449-475.

Sugawara, H., Yamamoto, H., Shihata, N., Inoue, T., Okada, S., Miyake, C., Yokota, A., and Kai, Y. (1999) Crystal structure of carboxylase reaction-oriented ribulose 1,5-bisphosphate carboxylase oxygenase from a thermophilic red alga, *Galdieria partita*. *J. Biol. Chem.* **274**:15655–15661.

Tabita, F.R. (1999) Microbial ribulose, 1,5-bisphosphate Carboxylase/oxygenase: A different perspective. *Photosynth. Res.* **60**:1-28.

Tabita, F.R., and Small, C.L. (1985) Expression and assembly of active cyanobacterial ribulose-1,5-bisphosphate carboxylase/oxygenase in Escherichia coli containing stoichiometric amounts of large and small subunits. *Proc. Natl. Acad. Sci.* **82**:6100-6103.

Tabita, F.R., Caruso, P., and Whitman, W. (1978) Facile assay of enzymes unique to the Calvin cycle in intact cells, with special reference to ribulose-1,5-bisphosphate carboxylase. *Anal. Biochem.* **84**:462-472.

Taylor, T.C., Backlund, A., Bjorhall, K., Spreitzer, R.J., and Andersson, I. (2001) First crystal structure of Rubisco from a green alga, *Chlamydomonas reinhardtii*. *J. Biol. Chem.* **276**:48159–48164.

Tcherkez, G., Farquhar, G., and Andrews, J. (2006) Despite slow catalysis and confused substrate specificity, all ribulose bisphosphate carboxylases may be nearly perfectly optimized. *Proc. Natl. Acad. Sci.* **103**:7246-7251.

Uemura, K., Anwarazzaman, M.S., and Yakota, A. (1997) Ribulose 1,5-bisphosphate carboxylase/oxygenase from thermophilic red algae with a strong specificity for CO2 fixation. *Biochem. Biophys. Res. Commun.* **233**: 568–571.

Watson, G.M., and Tabita, F.R. (1997) Microbial ribulose 1,5-bisphosphate carboxylase/oxygenase: a molecule for phylogenetic and enzymological investigation. *FEMS Microbiol. Lett.* **146**:13-22.

Watson, G., Yu, J., and Tabita, R. (1999) Unusual Ribulose 1,5-Bisphosphate Carboxylase/Oxygenase of Anoxic Archaea. *J. Bacteriol.* **181**:1569-1575.

Whitman, W., and Tabita, F.R. (1976) Inhibition of D-ribulose 1,5-bisphosphate carboxylase by pyridoxal 5'-

phosphate. *Biochem. Biophys. Res. Commun.* **71**:1034-1039.

Williams, K.A., and Deber, C.M. (1991) Proline residues in transmembrane helices: structural or dynamic role? *Biochemistry* **30**: 8919-8923.